Stability of superheavy nuclei produced in actinide-based complete fusion reactions: Evidence for the next magic proton number at $Z \geqslant 120$

G. G. Adamian,[1,2] N. V. Antonenko,[1] and V. V. Sargsyan[1,3]
[1] *Joint Institute for Nuclear Research, RU-141980 Dubna, Russia*
[2] *Institute of Nuclear Physics, Tashkent 702132, Uzbekistan*
[3] *Yerevan State University, Yerevan, Armenia*
(Received 31 December 2008; published 12 May 2009)

Using the experimental evaporation residue cross sections in the ^{48}Ca-induced complete fusion reactions and the complete fusion cross sections calculated within the dinuclear system model, the survival probabilities of superheavy nuclei with charge numbers $Z = 112$–116 and 118 in the xn-evaporation channels are extracted. The effects of angular momentum and deformations of colliding nuclei are taken into account. The obtained dependence of the survival probability on Z indicates the next doubly magic nucleus beyond ^{208}Pb at $Z \geqslant 120$.

DOI: 10.1103/PhysRevC.79.054608 PACS number(s): 25.70.Jj, 24.10.−i, 24.60.−k, 27.90.+b

I. INTRODUCTION

The experiments with the actinide-based complete fusion reactions ^{48}Ca + ^{233,238}U, ^{237}Np, ^{242,244}Pu, ^{243}Am, ^{245,248}Cm, ^{249}Cf were carried out at FLNR (Dubna), GSI (Darmstadt), and LBNL (Berkeley) [1–4] in order to approach to "the island of stability" of the superheavy elements (SHE) predicted at charge number $Z = 114$ and neutron number $N = 184$ with the macroscopic-microscopic models [5,6]. The found experimental trend of the nuclear properties (Q_α-values and half-lives) of the SHE produced in Dubna with ^{48}Ca-induced reactions reveals the increasing stability of nuclei approaching the spherical closed neutron shell $N = 184$, and also indicates a small influence of the proton shell at $Z = 114$. No discontinuity is observed yet when the proton number 114 is crossed at the neutron numbers 172 to 176 [4]. This experimental observation is in accordance with predictions of the relativistic and nonrelativistic mean field models [7] where the island of stability is near the nucleus with $Z = 120$–126 and $N = 184$. There is some hope to synthesize new SHE with $Z \geqslant 120$ by using the present experimental set up and the actinide-based reactions with neutron-rich stable projectiles heavier than ^{48}Ca.

The experimental evaporation residue cross sections σ_{xn} in the ^{48}Ca-induced complete fusion reactions do not depend strongly on the atomic number Z of SHE and are on the picobarn level. As known, the cross section of compound nucleus formation strongly decreases with increasing $Z_1 \times Z_2$. Since the absolute value of evaporation residue cross section is ruled by the product of complete fusion cross section and survival probability, the loss in the formation probability of compound nucleus in actinide-based reactions can be compensated by the gain in the survival probability of SHE. The aim of the present paper is to reveal the behavior of the survival probability with increasing Z of SHE by using the experimental evaporation residue cross sections and calculated fusion cross sections. Our study will indicate Z corresponding to the next spherical shell beyond ^{208}Pb.

II. METHOD

The cross section of the production of SHE as the evaporation residues in the xn-evaporation channel is written as a sum over all partial waves J

$$
\begin{aligned}
\sigma_{xn}(E_{\rm c.m.}) &= \sum_J \sigma_{\rm fus}(E_{\rm c.m.}, J) W_{xn}(E_{\rm c.m.}, J),\\
\sigma_{\rm fus}(E_{\rm c.m.}, J) &= \int_0^{\pi/2}\int_0^{\pi/2} d\cos\Theta_1 d\cos\Theta_2\\
&\quad \times \sigma_c(E_{\rm c.m.}, J, \Theta_i) P_{CN}(E_{\rm c.m.}, J, \Theta_i). \qquad (1)
\end{aligned}
$$

Here, the averaging over the orientations of statically deformed interacting nuclei [Θ_i ($i = 1,2$) are the orientation angles with respect to the collision axis] is taken into consideration. For the correct description of the experimental data, the partial capture cross section σ_c, fusion P_{CN}, and survival $W_{\rm sur}$ probabilities should be properly calculated [8–11]. The value of $\sigma_c(E_{\rm c.m.}, J, \Theta_i) = \frac{\pi\hbar^2}{2\mu E_{\rm c.m.}}(2J+1)T(E_{\rm c.m.}, J, \Theta_i)$ defines the transition of the colliding nuclei over the Coulomb barrier with the probability T and the formation of dinuclear system (DNS) when the kinetic energy $E_{\rm c.m.}$ and angular momentum J of the relative motion are transformed into the excitation energy and angular momentum of the DNS. The capture (transition) probability $T(E_{\rm c.m.}, J, (E_{\rm c.m.}, J)) = (1 + \exp[2\pi(V_J(R_b, \Theta_i) - E_{\rm c.m.})/\hbar\omega_J(\Theta_i)])^{-1}$ is calculated with the Hill-Wheeler formula. The effective nucleus-nucleus potential

$$V_J(R, \Theta_i) = V_N(R, \Theta_i) + V_C(R, \Theta_i) + \hbar^2 J(J+1)/(2\Im)$$

is calculated as a sum of nuclear V_N, Coulomb V_C, and centrifugal interactions [12] and approximated near the Coulomb barrier at $R = R_b$ by the inverted harmonic-oscillator potential with the barrier height $V_J(R_b, \Theta_i)$ and frequency $\omega_J(\Theta_i)$. In the entrance channel the moment of inertia is $\Im = \mu R^2$. The nuclear potential V_N is calculated with the double-folding model using a nuclear radius parameter $r_0 = 1.15$ fm and a diffuseness $a = 0.54$ fm for ^{48}Ca and $a = 0.56$ fm for the actinide targets [12]. The static quadrupole deformation parameters of

 ©2009 The American Physical Society

actinides are taken from Ref. [13]. Since the deformations of colliding nuclei influence here on the capture of the projectile by target at energies near the Coulomb barrier and the capture is rather fast process, the use of static deformations is quite justified. All potentials $V_J(R, \Theta_i)$ are calculated with the same set of the parameters and assumptions.

The DNS model [8–11] is successful in describing the complete fusion reactions especially related to the production of heavy and superheavy nuclei. In the DNS model the compound nucleus is reached by a series of transfers of nucleons from the light nucleus to the heavy one. The dynamics of the DNS is considered as a combined diffusion in the degrees of freedom of the mass asymmetry $\eta = (A_1 - A_2)/(A_1 + A_2)$ (A_1 and A_2 are the mass numbers of the DNS nuclei) and of the internuclear distance R. The diffusion in R occurs toward the values larger than the sum of the radii of the DNS nuclei and finally leads to the quasifission (decay of the DNS). After the capture stage, the probability of complete fusion

$$P_{CN} = \lambda_\eta^{Kr} / \left(\lambda_\eta^{Kr} + \lambda_{\eta_{\rm sym}}^{Kr} + \lambda_R^{Kr}\right)$$

depends on the competition between the complete fusion in η, diffusion in η to more symmetric DNS, and quasifission. This competition can strongly reduce the value of $\sigma_{\rm fus}(E_{\rm c.m.}, J)$ and, correspondingly, the value of $\sigma_{xn}(E_{\rm c.m.})$. Since the initial DNS is in the conditional minimum of potential energy surface, we use a two-dimensional (in η and R coordinates) Kramers-type expression for the quasistationary rates λ_η^{Kr} of fusion, $\lambda_{\eta_{\rm sym}}^{Kr}$ of symmetrization of the DNS, and λ_R^{Kr} of quasifission through the fusion barrier in η, the barrier in η toward symmetric DNS, and quasifission barrier in R, respectively. These barriers are given by the potential energy U of the DNS which is calculated as the sum of binding energies B_i of the DNS nuclei and of the nucleus-nucleus potential $V_J : U = B_1 + B_2 + V_J$. The binding energies for known and unknown nuclei are taken from Refs. [14] and [6] (the finite range droplet model), respectively. The uncertainty of calculated P_{CN} is within the factor of 2. The deformations of the DNS nuclei can deviate from their static values during the fusion process. Since the polarization effects in the DNS play a minor role in the dependence of U on the mass asymmetry, this deviation can be disregarded in the calculation of P_{CN}. The detailed description of the calculation procedure is given in Ref. [11].

The survival probability $W_{xn}(E_{\rm c.m.}, J)$ estimates the competition between fission and neutron evaporation in the excited compound nucleus. In expression (1) the contributing angular momentum range is limited by W_{xn}. In the case of highly fissile SHE, W_{xn} is a narrow function of J different from zero in the vicinity of $J = 0$ for all bombarding energies. The angular momentum dependence can be separated as

$$W_{xn}(E_{\rm c.m.}, J) = W_{xn}(E_{\rm c.m.}, J = 0) \exp\left[-\sum_{i=1}^{x} \frac{\Delta B_i^{\rm rot}}{T_i}\right] \approx W_{xn}(E_{\rm c.m.}, J = 0) \exp\left[-\frac{J^2}{J_m^2(x)}\right], \quad (2)$$

where $\Delta B_i^{\rm rot} = \hbar^2 J(J+1)[\frac{1}{2\theta_{\rm g.s.}^i} - \frac{1}{2\theta_{\rm s}^i}]$, $\theta_{\rm g.s.}^i$ ($\theta_{\rm s}^i$) is the moment of inertia in the ground state (at the saddle point) in ith evaporation step, $\theta_{\rm g.s.,s}^i \approx \theta_{\rm g.s.,s}^j \approx \theta_{\rm g.s.,s}$, $i \neq j$, $J_m(x) = \phi(x) J_m(x = 1)$, $J_m(x = 1) = (T_1/[\hbar^2/(2\theta_{\rm g.s.}) - \hbar^2/(2\theta_{\rm s})])^{1/2}$ (T_1 is the thermodynamical temperature in $1n$-channel) and $\phi(x) = (1 + \frac{1}{\sqrt{2}} + \cdots + \frac{1}{\sqrt{x}})^{-1}$. Since in heaviest nuclei the nuclear structure is drastically changed when the nucleus moves from the ground state to the saddle point, the values of $\theta_{\rm g.s.}^i$ and $\theta_{\rm s}^i$ are expected to be rather different in spite of small difference in the deformation parameters between the ground state and saddle point. Thus, $W_{xn}(E_{\rm c.m.}, J)$ is cut at higher angular momenta by a gaussian-like factor. The width of this cutoff $J_m(x)$ weakly decreases with increasing x. For the reactions leading to SHE, $J_m(x = 1) = 10$ is used at $E_{\rm c.m.}$ near the Coulomb barrier [10,11]. $J_m(x = 1) = 15$ was used in the actinide region [8]. These values of J_m correspond to the impact parameters less than 1 fm. In all heavy ion complete fusion reactions above the Coulomb barrier, we have $J_m < J_{\rm crit}$, where $J_{\rm crit}$ is the critical angular momentum which restricts the capture cross section. Therefore, only a limited part of the angular momentum distribution of compound nucleus appreciably contributes to the evaporation residue cross section.

Using Eqs. (1) and (2), and replacing the sum over J by the integral, we obtain the following approximate factorization:

$$\sigma_{xn}(E_{\rm c.m.}) = \sigma_{\rm fus}^{\rm eff}(E_{\rm c.m.}) W_{xn}(E_{\rm c.m.}, J = 0), \quad (3)$$

where

$$\sigma_{\rm fus}^{\rm eff}(E_{\rm c.m.}) = \frac{\pi\hbar^2}{\mu E_{\rm c.m.}} \int_0^\infty \int_0^{\pi/2} \int_0^{\pi/2} \times \frac{dJ d\cos\Theta_1 d\cos\Theta_2 \, J e^{-\frac{J^2}{J_m^2(x)}} P_{CN}(E_{\rm c.m.}, J, \Theta_i)}{1 + \exp[2\pi(V_J(R_b, \Theta_i) - E_{\rm c.m.})/\hbar\omega_J(\Theta_i)]} \quad (4)$$

is the effective fusion cross section because it contains the angular momentum dependence of survival probability. The uncertainty of $\sigma_{\rm fus}^{\rm eff}$ is mainly related to the uncertainty of the calculated value of P_{CN}. Using Eq. (3), one can extract the value of survival probability at the zero angular momentum from experimental cross section $\sigma_{xn}^{\rm exp}(E_{\rm c.m.})$ as

$$W_{xn}(E_{\rm c.m.}, J = 0) = \sigma_{xn}^{\rm exp}(E_{\rm c.m.}) / \sigma_{\rm fus}^{\rm eff}(E_{\rm c.m.}). \quad (5)$$

With the reduction to the zero angular momentum the survival probability becomes independent of the projectile-target combination.

III. EXTRACTION OF SURVIVAL PROBABILITIES FROM EXPERIMENTAL CROSS SECTIONS

To deduce the "experimental" value of the survival probability of SHE it is necessary to calculate the effective fusion cross section $\sigma_{\rm fus}^{\rm eff}(E_{\rm c.m.})$. The fusion probability and, correspondingly, the effective fusion cross section $\sigma_{\rm fus}^{\rm eff}(E_{\rm c.m.})$ decreases by about 2 orders of magnitude with increasing the charge number of compound nucleus from $Z = 112$ to $Z = 118$ (Fig. 1). The fusion hindrance is due to a strong competition between complete fusion and quasifission in the DNS. The contribution of quasifission to the reaction cross section strongly increases with Z due to the increasing Coulomb

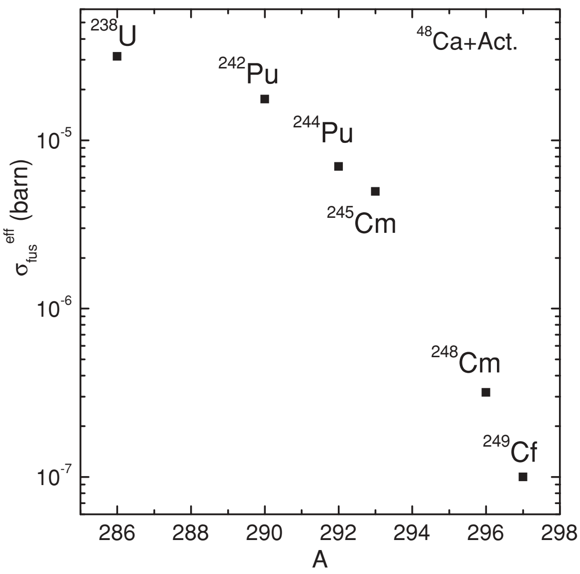

FIG. 1. Effective fusion cross section as a function of mass number of the compound nucleus in ^{48}Ca-induced complete fusion reactions at bombarding energies supplying the maximal yield of evaporation residues in $3n$-channel. The actinide targets are indicated.

repulsion in the DNS. As seen in Fig. 1, the cross section of compound nucleus formation in the ^{48}Ca-induced reactions with actinide targets is substantially higher than the evaporation residue cross section reduced by the survival probability.

In Fig. 2 the extracted values of W_{3n} and W_{4n} with Eq. (5) deviate from the expected magic proton number $Z = 114$. This indicates an increase of the stability of SHE beyond $Z = 114$. The experimental error-bars result the error-bars in the deduced W_{xn}. Since the fission barrier is determined by the shell correction energy, the absolute value of the shell correction energy is expected to be increased with Z. The shell correction energy strongly depends on that how the neutron and proton numbers of the compound nucleus are close to the magic proton and neutron numbers. The found experimental trend of the Q_α-values in α-decay chains also indicates the monotonic increase of the amplitude of the ground state shell correction energy with charge number in the region $Z = 112$–118 [4]. One can expect the increasing stability of nuclei approaching the closed neutron $N = 184$ shell. However, in Fig. 2 $W_{3n}(^{296}_{180}116) < W_{3n}(^{297}_{179}118)$. This probably indicates that $Z = 114$ is not a proper proton magic number and the next doubly magic nucleus beyond ^{208}Pb is the nucleus with $Z \geqslant 120$. The shell closure at $Z \geqslant 120$ may influence stronger on the stability of the SHE than the sub-shell closure at $Z = 114$. Note that the experimental uncertainties seem to be too small to overcome the trends presented in Fig. 2.

Figures 3–5 show the dependencies of W_{xn} on the excitation energy of compound nucleus for different SHE. For the compound nucleus ^{286}112 (^{290}114) the maximal W_{3n} is about

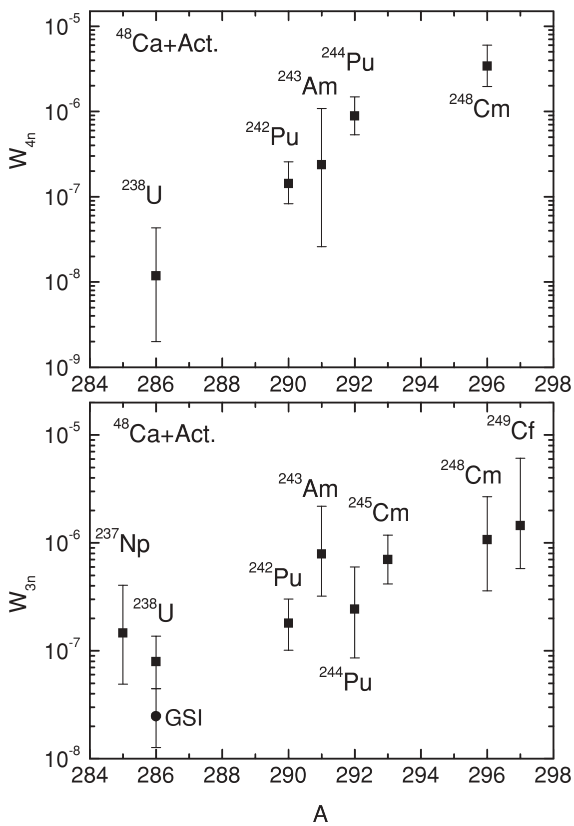

FIG. 2. The survival probabilities of SHE in $3n$-and $4n$-channels, extracted with Eq. (5) and experimental σ_{xn}^{exp} from Refs. [1], as functions of mass number of the compound nucleus. For the reaction ^{48}Ca + ^{238}U, the experimental σ_{3n}^{exp} from GSI [4] is used as well.

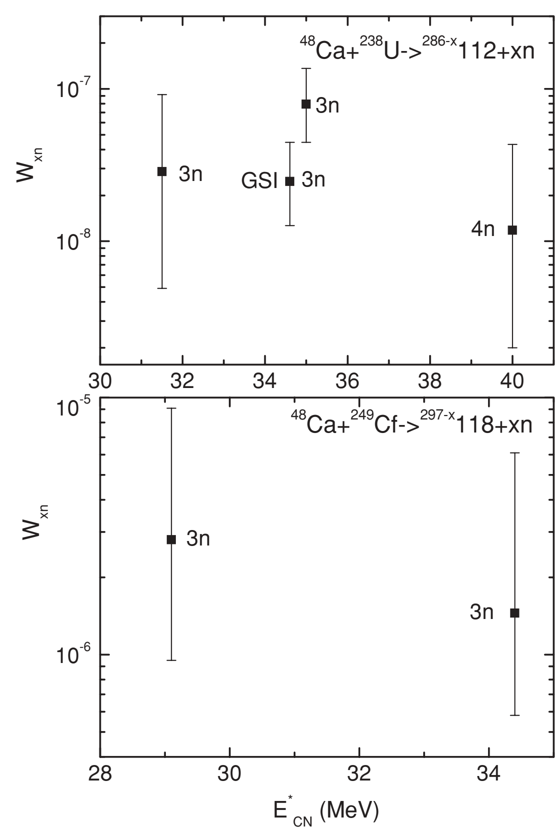

FIG. 3. The survival probabilities of compound nuclei ^{286}112 and ^{297}118 in the indicated xn-channels as functions of excitation energy calculated with the mass table of Ref. [15].

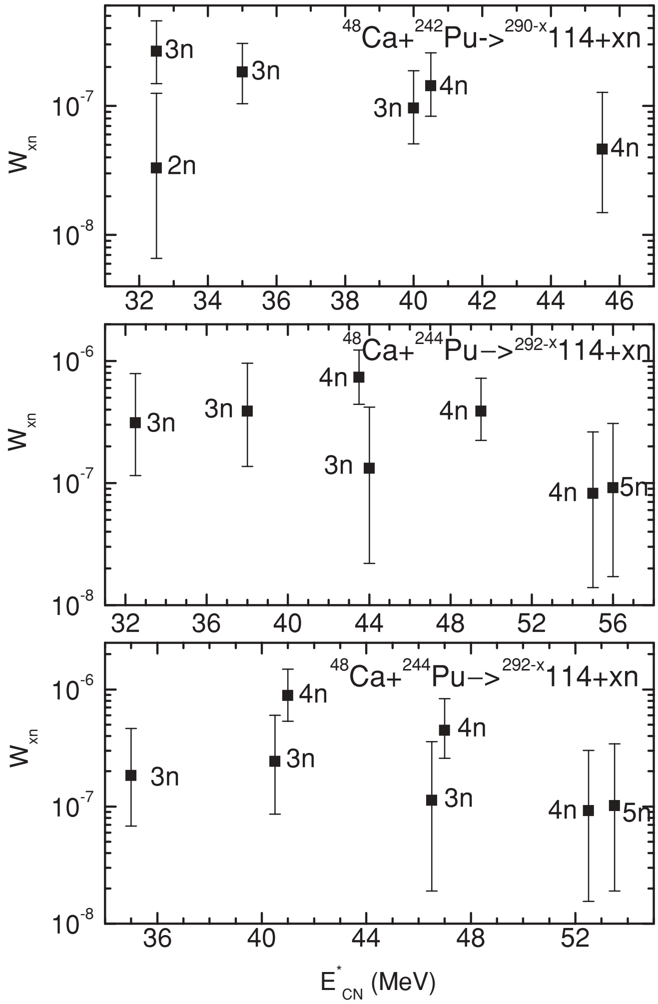

FIG. 4. The same as in Fig. 3, but for the compound nuclei $^{290}114$ and $^{292}114$. In the middle part the experimental energies are shifted by ±2.5 MeV (see text).

7 (2) times larger than W_{4n}. In contrast, for the compound nucleus $^{292}114$ ($^{296}116$) the maximal W_{3n} is about 3 (2) times smaller than W_{4n}. One can understand this if the excitation energies are not optimal for the $3n$-evaporation channel. Besides the uncertainty in absolute value of the production cross section, there is the experimental uncertainty of about 5 MeV in the definition of E^*_{CN}. To demonstrate the sensitivity of the ratio between the extracted W_{3n} and W_{4n} to the uncertainty of E^*_{CN}, for nucleus $^{292}114$ we shifted the excitation energies by −2.5 MeV in $3n$-channel and by +2.5 MeV in $4n$-and $5n$-channels. As seen in Fig. 5, the absolute values of W_{3n} become closer to the values of W_{4n} in this case. Note that the results of Figs. 3–5 are weakly sensitive to the reasonable variation of J_m in Eq. (3).

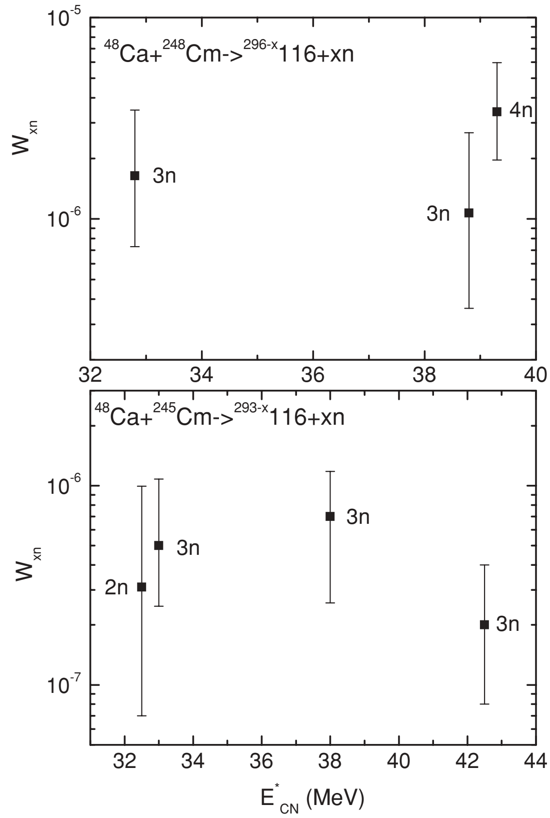

FIG. 5. The same as in Fig. 3, but for the compound nuclei $^{295}116$ and $^{298}116$.

IV. SUMMARY

The found enhancement of W_{xn} with increasing charge number of the SHE from $Z = 114$ to 118 indicates that the ground state shell corrections growth with Z. Thus, the present experimental data point out that a magic proton shell is at $Z \geqslant 120$.

ACKNOWLEDGMENTS

This work was supported by DFG and RFBR. The IN2P3-JINR and Polish-JINR Cooperation programs are gratefully acknowledged.

[1] Yu. Ts. Oganessian, J. Phys. G **34**, R165 (2007).
[2] W. Loveland *et al.*, Phys. Rev. C **66**, 044617 (2002); K. E. Gregorich *et al.*, *ibid.* **72**, 014605 (2005).
[3] A. B. Yakushev *et al.*, Radiochimica Acta **91**, 433 (2003); R. Eichler *et al.*, Nature (London) **447**, 72 (2007).
[4] S. Hofmann *et al.*, Eur. Phys. J. A **32**, 251 (2007).
[5] S. Hofmann and G. Münzenberg, Rev. Mod. Phys. **72**, 733 (2000).
[6] P. Möller *et al.*, At. Data Nucl. Data Tables **59**, 185 (1995).
[7] M. Bender *et al.*, Phys. Lett. **B515**, 42 (2001); P. Ring, Prog. Part. Nucl. Phys. **37**, 193 (1996); S. Cwiok *et al.*, Nucl. Phys. **A611**, 211 (1996); M. Bender, P. H. Heenen, and P. G. Reinhard, Rev. Mod. Phys. **75**, 121 (2003).
[8] N. V. Antonenko, E. A. Cherepanov, A. K. Nasirov, V. P. Permjakov, and V. V. Volkov, Phys. Lett. **B319**, 425 (1993); Phys. Rev. C **51**, 2635 (1995); V. V. Volkov, Phys. Part. Nucl. **35**, 797 (2004).

[9] G. G. Adamian, N. V. Antonenko, W. Scheid, and V. V. Volkov, Nucl. Phys. **A633**, 409 (1998); Nuovo Cimento A **110**, 1143 (1997); R. V. Jolos, A. I. Muminov, and A. K. Nasirov, Eur. Phys. J. A **4**, 245 (1999); E. A. Cherepanov, JINR Report No. E7-99-27, 1999; G. Giardina, S. Hofmann, M. I. Muminov, and A. K. Nasirov, Eur. Phys. J. A **8**, 205 (2000); G. G. Adamian, N. V. Antonenko, and W. Scheid, Nucl. Phys. **A678**, 24 (2000); Phys. Rev. C **68**, 034601 (2003); G. G. Adamian and N. V. Antonenko, Phys. Rev. C **72**, 064617 (2005).

[10] A. S. Zubov, G. G. Adamian, N. V. Antonenko, S. P. Ivanova, and W. Scheid, Phys. Rev. C **65**, 024308 (2002); **68**, 014616 (2003); G. G. Adamian, N. V. Antonenko, and A. S. Zubov, *ibid.* **71**, 034603 (2005).

[11] G. G. Adamian, N. V. Antonenko, and W. Scheid, Phys. Rev. C **69**, 014607 (2004); **69**, 044601 (2004).

[12] G. G. Adamian *et al.*, Int. J. Mod. Phys. E **5**, 191 (1996).

[13] S. Raman, C. W. Nestor, and P. Tikkanen, At. Data Nucl. Data Tables **78**, 1 (2001).

[14] G. Audi and A. H. Wapstra, Nucl. Phys. **A565**, 1 (1993).

[15] W. D. Myers and W. J. Swiatecki, Nucl. Phys. **A601**, 141 (1996).